

## Superconducting Behavior in Compressed Solid SiH<sub>4</sub> with a Layered Structure

Xiao-Jia Chen,<sup>1,2,3</sup> Jiang-Long Wang,<sup>1</sup> Viktor V. Struzhkin,<sup>2</sup> Ho-kwang Mao,<sup>2</sup> Russell J. Hemley,<sup>2</sup> and Hai-Qing Lin<sup>1</sup>

<sup>1</sup>*Department of Physics and ITP, Chinese University of Hong Kong, Hong Kong, China*

<sup>2</sup>*Geophysical Laboratory, Carnegie Institution of Washington, Washington, D.C. 20015, USA*

<sup>3</sup>*School of Physics, South China University of Technology, Guangzhou 510640, China*

(Received 19 June 2007; published 12 August 2008)

The electronic and lattice dynamical properties of compressed solid SiH<sub>4</sub> have been calculated in the pressure range up to 300 GPa with density functional theory. We find two energetically preferred insulating phases with  $P2_1/c$  and  $Fdd2$  symmetries at low pressures. We demonstrate that the  $Cmca$  structure having a layered network is the most likely candidate of the metallic phase of SiH<sub>4</sub> over a wide pressure range above 60 GPa. The superconducting transition temperature in this layered metallic phase is found to be in the range of 20–75 K.

DOI: [10.1103/PhysRevLett.101.077002](https://doi.org/10.1103/PhysRevLett.101.077002)

PACS numbers: 74.10.+v, 74.25.Jb, 74.62.Fj

SiH<sub>4</sub> offers a source for high purity silicon in epitaxial and thin film deposition which is at the base of electronics and microdevices. There is ongoing interest in this material as well due to the suggestion of Ashcroft [1] that SiH<sub>4</sub> would eventually undergo a transition to metallic and then a superconducting state at pressures considerably lower than may be necessary for solid hydrogen. Exploring the possibility of metallic hydrogen has long been a major driving force in high-pressure condensed matter science and remains an important challenge in modern physics and astrophysics [2]. Recent experimental work on SiH<sub>4</sub>, using diamond-anvil cell techniques, has revealed an enhanced reflectivity with increasing pressure [3,4]. It was found [4] that solid SiH<sub>4</sub> becomes opaque at 27–30 GPa and exhibits Drude-like behavior at around 60 GPa, signalling the onset of pressure-induced metallization. Structural information is the primary step toward understanding these observed electronic properties.

SiH<sub>4</sub> has a rich phase diagram with at least seven known phases [4–6]. Only one solid phase has been reported in the pressure range between 10 and 25 GPa and at room temperature, with a monoclinic structure (space group  $P2_1/c$ ) [7]. The very low hydrogen scattering cross section of hydrogen-containing materials in most diffraction methods makes structural determination very difficult, specifically in determining the H positions, and the neutron diffraction technique is limited to 30 GPa [8]. The challenge of experimentally or theoretically determining the high-pressure structures of SiH<sub>4</sub> is still enormous.

The sequence of SiH<sub>4</sub> structures provides the basis for understanding whether the material is a favorable candidate of a high-temperature superconductor [9]. Currently, there has been much effort in searching for possible candidate structures of this material on the basis of the first-principles density functional theory which has proved an efficient means of calculating quite accurate energies. For a metallic  $Pman$  SiH<sub>4</sub> phase, Feng *et al.* [10] obtained a superconducting transition temperature  $T_c$  of 166 K at 202 GPa by using the electron-phonon coupling strength for lead under ambient pressure as both materials have the

same characteristic density of states per volume at relevant pressures. Pickard and Needs [11] also studied the structural properties of SiH<sub>4</sub> and mentioned the possibility of superconductivity in a  $C2/c$  phase. All previous work [7,10,11] was done without including the calculations of the phonon spectra and electron-phonon coupling parameters. Later phonon calculations by Yao *et al.* [12] showed that the  $Pman$  structure is in reality not stable and that a new  $C2/c$  structure is dynamically stable from 65 to 150 GPa. This  $C2/c$  SiH<sub>4</sub> phase was predicted to exhibit superconductivity close to 50 K at 125 GPa [12]. The identification of high-pressure structures of SiH<sub>4</sub> is still a matter of debate, and no study on superconductivity with other stable structures has been attempted.

In this Letter, we report a theoretical study of structural, electronic, vibrational, and superconducting properties of solid SiH<sub>4</sub> at high pressures. We find two insulating phases  $P2_1/c$  and  $Fdd2$  at low pressures and identify the layered  $Cmca$  structure as the most likely metallic phase of SiH<sub>4</sub>, with a superconducting transition temperature in the range of 20–75 K.

To study the structural and electronic behavior of SiH<sub>4</sub> over a wide range of pressure, we used the Perdew-Burke-Ernzerhof generalized gradient approximation (GGA) density functional and projector augmented wave method as implemented in the Vienna *ab initio* simulation package (VASP) [13]. An energy cutoff of 450 eV is used for the plane wave basis sets, and  $16 \times 16 \times 16$  and  $8 \times 8 \times 8$  Monkhorst-Pack  $k$ -point grids are used for Brillouin zone sampling of two SiH<sub>4</sub> molecular cells and four SiH<sub>4</sub> molecular cells, respectively. The lattice dynamical and superconducting properties were calculated by the QUANTUM-ESPRESSO package [14] using Vanderbilt-type ultrasoft potentials with a cutoff energy of 25 and 200 Ry for the wave functions and the charge density, respectively.  $12 \times 12 \times 12$  Monkhorst-Pack  $k$ -point grids with Gaussian smearing of 0.02 Ry were used for the phonon calculations at  $4 \times 4 \times 4$   $q$ -point mesh, and double  $k$ -point grids were used for calculation of the electron-phonon interaction matrix element.

We performed a systematic study of the phase stability of  $\text{SiH}_4$  based on *ab initio* first-principles calculations. Out of more than 100 structures that we studied, six new polymorphs of  $\text{SiH}_4$  with low enthalpies are found in the pressure range from 0 to 300 GPa. In Fig. 1, we plot the pressure dependence of their enthalpies along with the results for the  $C2/c$  and  $I4_1/a$  structure reported previously [11]. A monoclinic structure with  $P2_1/c$  symmetry has the lowest enthalpy below 27 GPa, in good agreement with the recent experiments [7]. The  $P2_1/c$  structure consists of four isolated covalently bonded  $\text{SiH}_4$  tetrahedra with the H atom of one molecule pointing away from the H atoms of a neighboring molecule. We find that a face-centered orthorhombic structure with  $Fdd2$  symmetry appears stable from 27 to 60 GPa. These two phases are insulating.

Near 50 GPa, there are three other competitive, low-enthalpy structures with the  $C2/c$ ,  $I4_1/amd$ , and  $I4_1/a$  symmetry. Our  $C2/c$  structure was based on the  $\text{UI}_4$  arrangement, which exhibits a layered structure. However, the  $C2/c$  structure predicted by Pickard and Needs [11] forms three-dimensional networks at high pressures. For clarification, we name their structure as  $C2/c$  (3D) and our layered structure as  $C2/c$  (2D). There are subtle differences in band structures between the  $C2/c$  predicted by Yao *et al.* [12] and our  $C2/c$  (2D). Our  $C2/c$  (2D) structure is composed of sixfold-coordinated  $\text{SiH}_6$  octahedra inside a layer, but Si-H bonding between different layers is absent. It is still dynamically stable up to 250 GPa. However, the stability of the  $C2/c$  phase of Yao *et al.* [12] is stable only up to 150 GPa. On compression, the sixfold-coordinated  $\text{SiH}_6$  octahedra are transformed into eightfold-coordinated  $\text{SiH}_8$  dodecahedra with a  $\text{S}_2\text{H}_2$  bridgelike bonding arrangement within the layer. Above 110 GPa, the  $C2/c$  (2D) structure becomes metallic. The  $I4_1/amd$   $\text{SiH}_4$  phase is composed of eightfold-coordinated  $\text{SiH}_8$  dodecahedra, and every Si atom shares two H atoms with other Si atoms, as in the  $I4_1/a$  structure. The

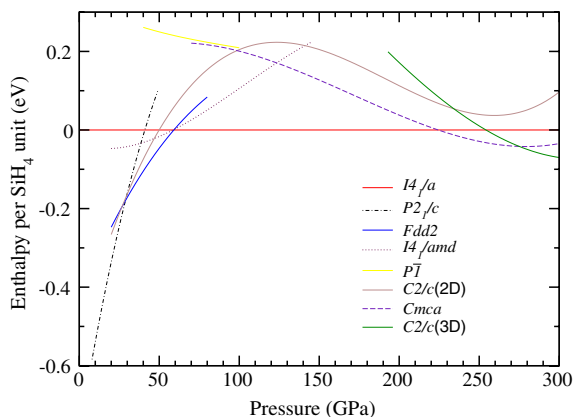


FIG. 1 (color online). The enthalpy versus pressure for competitive structures of  $\text{SiH}_4$ . The enthalpy of the  $I4_1/a$  phase is taken as the reference point.

$I4_1/amd$ -type  $\text{SiH}_4$  is a semimetal between 40 and 70 GPa.

The  $I4_1/a$  structure was found to have the lowest enthalpy over a wide pressure range (60–220 GPa), consistent with previous calculations [11]. In an early powder x-ray diffraction study [15],  $I4_1/a$  was considered as one of most plausible structures for the low-temperature phase II. Raman measurements [4] indicate that this structure may not exist for  $\text{SiH}_4$  under high pressure and at room temperature.  $\text{SiH}_4$  in the  $I4_1/a$  structure is believed to be stable only at low temperature. Between 220 and 270 GPa, a metallic  $Cmca$  structure has the lowest enthalpy. Upon further compression, the  $C2/c$  (3D) phase possesses the lowest enthalpy between 270 and 300 GPa, which confirms the previous calculations [11]. The  $Cmca$  phase is also a layered structure that consists of eightfold-coordinated  $\text{SiH}_8$  dodecahedra. In each layer, the Si-H bonding arrangement is the same as that in the  $I4_1/a$  structure. Thus, the  $Cmca$  phase can be viewed as the 2D analogue of the  $I4_1/a$  phase.

In the 60–100 GPa range, we found a metallic triclinic structure with a  $P\bar{1}$  space group with eightfold  $\text{SiH}_8$  coordination. It has almost the same enthalpy as the  $Cmca$  structure between 60 and 100 GPa. Both of their enthalpies are within 0.25 eV of the insulating  $I4_1/a$  structure. The enthalpic difference between them and  $I4_1/a$  is reduced with increasing pressure. We thus obtain six energetically favorable structures for  $\text{SiH}_4$  at high pressures. The atomic arrangement for each of these structures is shown in Fig. 2. The  $P\bar{1}$ ,  $Cmca$ , and  $C2/c$  (2D) phases have layered structures and are metallic. Experimentally, the emergence of a metallic phase of  $\text{SiH}_4$  was reported for pressures just above 60 GPa [4]. The theoretically obtained insulating  $I4_1/a$  phase as the ground state is in contradiction to experiment. This is probably due to temperature effects (total energy calculations correspond to the zero temperature enthalpy) or a slight failure of the GGA approximation. We also should mention that the enthalpic contributions from electron-phonon coupling were not included when determining structure. The electron-phonon coupling was assumed to have negligible and similar effects on enthalpy for different structure. This may shift the pressure at which structure transform occurs, but the overall picture of the phase diagram is believed to remain unchanged. The enthalpy of the metallic  $Cmca$  could be lowered if we would include enthalpic contributions from electron-phonon coupling because it plays an important role in superconductivity (discussion below).

As the 2D analogue of  $I4_1/a$ , the metallic  $Cmca$  has comparable enthalpy to  $I4_1/a$  over the pressure range from 60 to 220 GPa, but it possesses the lowest enthalpy at higher pressures. Although the experimentally observed x-ray diffraction patterns have been refined as the  $P6_3$  structure [9], we found that the  $P6_3$  has relatively high enthalpy compared to the  $Cmca$ . Phonon calculations further reveal that the  $P6_3$  is a dynamically unstable state.

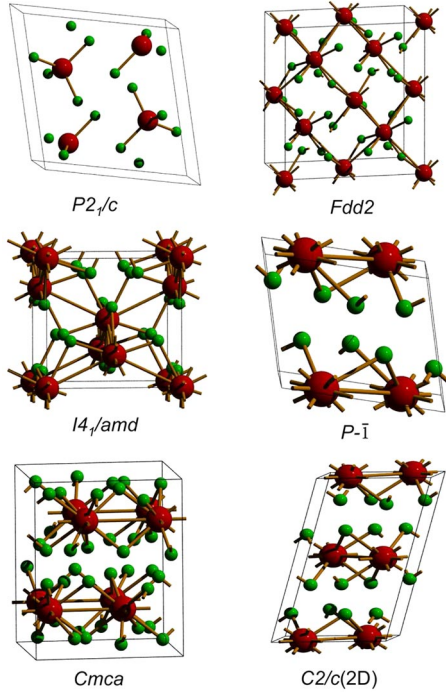


FIG. 2 (color online). The energetically most favorable structures computed for  $\text{SiH}_4$  polymorphs at various pressures.

Consequently, it can be concluded that the most likely candidate for the metallic  $\text{SiH}_4$  is the  $Cmca$  phase.

We now discuss the electronic, phononic, and superconducting properties of the metallic  $\text{SiH}_4$  with  $Cmca$  symmetry. Figure 3(a) shows the calculated band structure for the  $Cmca$   $\text{SiH}_4$  at 250 GPa. It can be seen that the  $Cmca$  structure is metallic. The valence bands cross the Fermi level  $E_F$  along the  $Y\Gamma$  direction, while the conduction bands cross  $E_F$  near the  $\Gamma$  point. Upon compression, the conduction band crossing across  $E_F$  at the  $\Gamma$  point shifts lower in energy, while the valence band across  $E_F$  along the  $Y\Gamma$  direction only moves up slightly in energy. The net effect of the pressure-induced band shifts is to increase the volume of the Fermi surface and the phase space for the electron-phonon interaction. Note that there exists a platform near the Fermi level along  $Y\Gamma$  direction. This is also a characteristic of layered cuprate superconductors. The flat band at the Fermi level will result in a large density of states, which in turn could lead to high- $T_c$  superconductivity.

The structural stability of the  $Cmca$   $\text{SiH}_4$  phase has been examined through lattice dynamics calculations. The typical results of the phonon dispersion and projected phonon density of states at pressure of 250 GPa are displayed in Fig. 3(b). The  $Cmca$  stability is confirmed by the absence of imaginary frequency modes. There are weak interactions between the Si framework and H atoms over the whole frequency range. The heavy Si atoms dominate the low-frequency vibrations, and the light H atoms contribute significantly to the high-frequency modes. Three separate regions of bands can be recognized. The modes for the

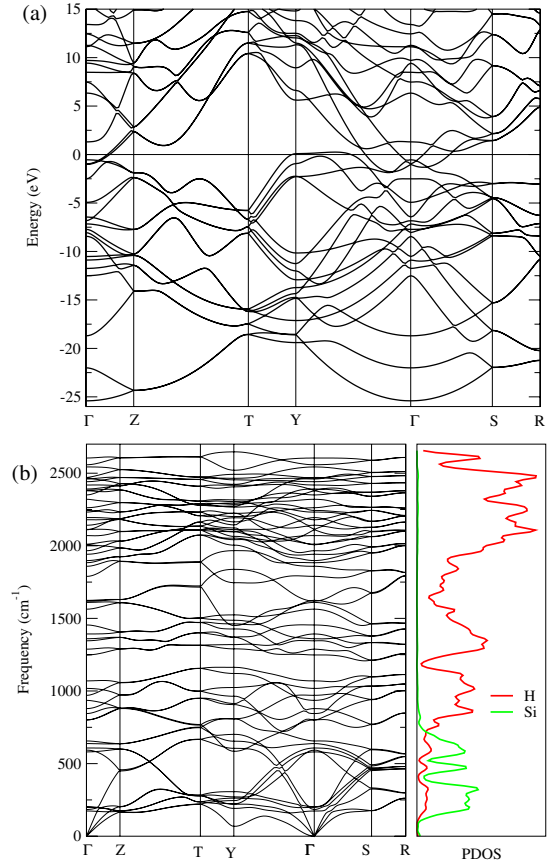


FIG. 3 (color online). (a) Electronic band structure for the  $Cmca$   $\text{SiH}_4$  phase at 250 GPa. The horizontal line shows the location of the Fermi level. (b) The phonon dispersion and phonon density of states (PDOS) projected on Si and H atoms for the  $Cmca$   $\text{SiH}_4$  at 250 GPa.

frequencies below  $750 \text{ cm}^{-1}$  are mainly due to the motions of Si. The bands around  $200 \text{ cm}^{-1}$  are caused by acoustic phonons. The Si-H-Si bending vibrations dominate the intermediate-frequency region between  $750$  and  $1200 \text{ cm}^{-1}$ . At high frequencies above  $1200 \text{ cm}^{-1}$ , the phonon spectrum belongs to the Si-H bond stretching vibrations.

The electron-phonon spectral function  $\alpha^2F(\omega)$  is essential in determining the electron-phonon coupling strength  $\lambda$  and logarithmic average phonon frequency  $\omega_{\log}$ . We have calculated  $\alpha^2F(\omega)$  for the metallic  $\text{SiH}_4$  phases in the pressure range of interest. Figure 4 shows the results for the  $Cmca$   $\text{SiH}_4$ . Below  $600 \text{ cm}^{-1}$ , the major contributions to  $\alpha^2F(\omega)$  come from the phonon modes involving Si-Si vibrations, and the remaining part of the electron-phonon coupling is mainly due to the phonon modes involving H-H vibrations. The  $\alpha^2F(\omega)$  on the wide high-energy side is significantly higher than that on the narrow low-energy side. Thus the high-energy H-H vibrations dominate the total  $\lambda$  value. Among the pressure levels considered, the  $Cmca$  phase at 70 GPa has a relatively large  $\alpha^2F(\omega)$  over the frequency range from  $700$  to  $1700 \text{ cm}^{-1}$ , resulting in a large  $\lambda$ .

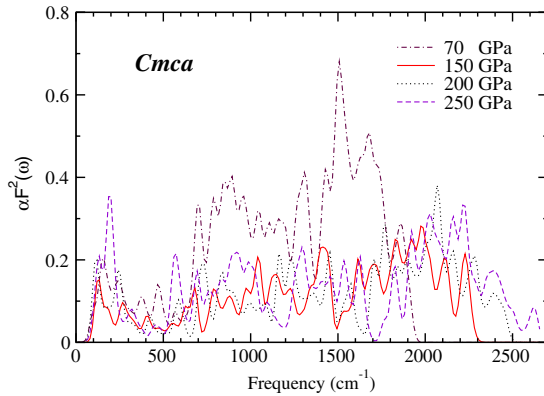


FIG. 4 (color online). Electron-phonon spectral function  $\alpha^2 F(\omega)$  versus frequency  $\omega$  of the *Cmca* SiH<sub>4</sub> at pressures.

We next examine the superconductivity in the metallic SiH<sub>4</sub> with *Cmca* structure, using the  $T_c$  equation derived by Allen and Dynes [16]. In the calculations, we took the Coulomb pseudopotential  $\mu^*$  to be 0.1, which was found to reproduce  $T_c$  in MgB<sub>2</sub> [17]. Figure 5 shows the pressure dependence of  $\omega_{\log}$ ,  $\lambda$ , and  $T_c$  for the *Cmca* SiH<sub>4</sub>. The calculated  $\omega_{\log}$  and  $\lambda$  do not show a monotonic pressure dependence. The variation of  $T_c$  with pressure is found to resemble the  $\lambda$  behavior, decreasing with increasing pressure but increasing upon further compression after passing a minimum value of  $\sim 20$  K at 150 GPa. This behavior is very similar to the experiments [9], though the magnitude of  $T_c$  is different. It should be mentioned that the Coulomb pseudopotential may affect the estimation of  $T_c$ . In hydrogen-dominant alloys, the phonon energy is usually a larger fraction of the Fermi energy than in most metals, and this tends to enhance  $\mu^*$ . We have gotten a slightly smaller value of  $T_c$  when using a larger  $\mu^*$  of 0.12, yielding the correct tendency of  $T_c$  as experimentally observed. For hydrogen-rich material like SiH<sub>4</sub>, we believe that a choice of  $\mu^*$  in the range of 0.09–0.12 would capture the basic

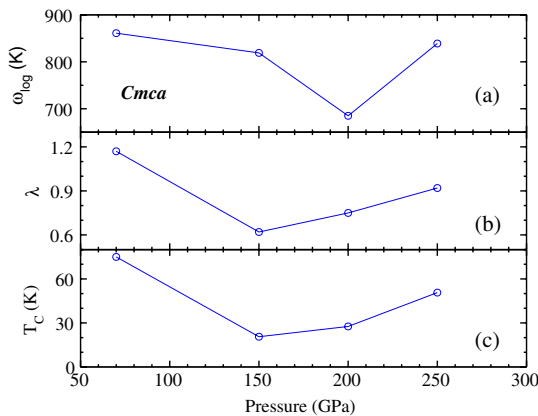


FIG. 5 (color online). Calculated (a) logarithmic average phonon frequency  $\omega_{\log}$ , (b) electron-phonon coupling parameter  $\lambda$ , and (c) superconducting transition temperature  $T_c$  of the *Cmca* phase of metallic SiH<sub>4</sub> as a function of pressure.

physics. In fact, typical values of  $\mu^*$  have been confirmed to be in the vicinity of 0.1 at least for high density systems [18].

In summary, we have investigated the structural stability of silane under pressure up to 300 GPa. The  $P2_1/c$  phase is confirmed to be a good candidate for the low-pressure insulating phase. Between 27 and 60 GPa, *Fdd2* is predicted to be the structure of another insulating phase. At higher pressures, the *Cmca* is proposed to be the most likely candidate of the metallic phase of SiH<sub>4</sub>. The superconductivity of the *Cmca* phase with a transition temperature ranging from 20 to 75 K is found to be mainly attributed to the strong electron-phonon coupling due to the phonon modes involving H-H vibrations.

We are grateful to J.S. Tse, R.E. Cohen, and S.A. Gramsch for discussions. This work was supported by Grants No. HKRGC-402205, No. DEFG02-02ER34P5, No. DEFC03-03NA00144, and No. DMR-0205899. X.-J.C. thanks CUHK for kind hospitality during the course of this work.

- [1] N. W. Ashcroft, Phys. Rev. Lett. **92**, 187002 (2004).
- [2] V. L. Ginzburg, Rev. Mod. Phys. **76**, 981 (2004).
- [3] L. L. Sun, A. L. Ruoff, C. S. Zha, and G. Stupian, J. Phys. Condens. Matter **18**, 8573 (2006); **19**, 479001 (2007).
- [4] X. J. Chen, V. V. Struzhkin, Y. Song, A. F. Goncharov, M. Ahart, Z. X. Liu, H. K. Mao, and R. J. Hemley, Proc. Natl. Acad. Sci. U.S.A. **105**, 20 (2008).
- [5] K. Clusius, Z. Phys. Chem., Abt. B **23**, 213 (1933).
- [6] R. E. Wilde and T. K. K. Srinivasan, J. Phys. Chem. Solids **36**, 119 (1975).
- [7] O. Degtyareva, M. Martinez-Canales, A. Bergara, X. J. Chen, Y. Song, V. V. Struzhkin, H. K. Mao, and R. J. Hemley, Phys. Rev. B **76**, 064123 (2007).
- [8] Y. Ding, J. Xu, C. T. Prewitt, R. J. Hemley, H. K. Mao, J. A. Cowan, J. Z. Zhang, J. Qian, S. C. Vogel, K. Lokshin, and Y. S. Zhao, Appl. Phys. Lett. **86**, 052505 (2005).
- [9] After submission of the present work, evidence for superconductivity in metallic silane was reported [M. I. Eremets *et al.*, Science **319**, 1506 (2008)].
- [10] J. Feng, W. Grochala, T. Jaroń, R. Hoffmann, A. Bergara, and N. W. Ashcroft, Phys. Rev. Lett. **96**, 017006 (2006).
- [11] C. J. Pickard and R. J. Needs, Phys. Rev. Lett. **97**, 045504 (2006).
- [12] Y. Yao, J. S. Tse, Y. Ma, and K. Tanaka, Europhys. Lett. **78**, 37003 (2007).
- [13] G. Kresse and J. Furthmuller, Comput. Mater. Sci. **6**, 15 (1996).
- [14] See <http://www.pwscf.org>; also S. Baroni, S. de Gironcoli, A. Dal Corso, and P. Giannozzi, Rev. Mod. Phys. **73**, 515 (2001).
- [15] W. M. Sears and J. A. Morrison, J. Chem. Phys. **62**, 2736 (1975).
- [16] P. B. Allen and R. C. Dynes, Phys. Rev. B **12**, 905 (1975).
- [17] P. P. Singh, Phys. Rev. Lett. **97**, 247002 (2006).
- [18] C. F. Richardson and N. W. Ashcroft, Phys. Rev. Lett. **78**, 118 (1997).